The lattice dynamics of forsterite

GEOFFREY D. PRICE

Department of Geological Sciences, University College London, Gower St, London WC1E 6BT

STEPHEN C. PARKER

School of Chemistry, University of Bath, Bath BA2 7AY

AND

MAURICE LESLIE

SERC Daresbury Laboratory, Daresbury, Warrington WA4 4AD

Abstract

We use an approach based upon the atomistic or Born model of solids, in which potential functions represent the interactions between atoms in a structure, to calculate the infrared and Raman vibrational frequencies of forsterite. We investigate a variety of interatomic potentials, and find that although all the potentials used reproduce the structural and elastic behaviour of forsterite, only one potential (THB1) accurately predicts its lattice dynamics. This potential includes 'bond-bending' terms, that model the directionality of the Si–O bond, which we suggest plays a major role in determining the structural and physical properties of silicates. The potential was derived empirically from the structural and physical data of simple oxides, and its ability to model the lattice dynamics of forsterite is a significant advance over previous, force-constant models, which have been simply derived by fitting to the spectroscopic data that they aim to model. The success that we have had in predicting the lattice dynamics of forsterite indicates that the potential provides the previously elusive yet fundamental, quantitative link between the microscopic or atomistic behaviour of a mineral and its macroscopic or bulk thermodynamic properties.

KEYWORDS: atomistic model, Born model, lattice dynamics, forsterite.

Introduction

ONE of the fundamental aims of mineralogical research is to determine which minerals exist under given pressure, temperature, and compositional conditions, and to understand why those specific minerals are more stable than any others. In an attempt to assess how close mineralogical research is to achieving this ultimate goal, Kieffer and Navrotsky (1985) presented a volume which stressed that the full understanding of the macroscopic behaviour of minerals, and eventually rocks, can only be obtained from a detailed knowledge of their microscopic or atomistic nature. This microscopic understanding is required because it is the response at the atomic level to changes in pressure and temperature that eventually determines the bulk properties of a material. The link between the microscopic properties of materials and their macroscopic behaviour is best made via their vibrational spectra, because such spectra are both determined by interatomic interactions, and are directly related to many bulk thermodynamic properties such as heat capacity, entropy, etc. (see for example McMillan, 1985; Kieffer, 1985). If, therefore, we wish to understand from first principles the behaviour and properties of Earth-forming minerals, we must be able to predict and rationalise their lattice vibrations—or equivalently their infrared and Raman spectra and phonon dispersion curves.

The frequencies of atomic vibrations within a crystal are determined by the strength and nature of the bonding which holds the atoms in that crystal together. More generally, these bonding forces can be described in terms of interatomic potentials, which not only determine the vibrational characteristics of a crystal but also its structure and physical properties, such as its elastic and dielectric behaviour. Because the vibrational behaviour of a

Mineralogical Magazine, March 1987, Vol. 51, pp. 157–70

material provides this vital link between its internal bonding and thermodynamic behaviour, considerable effort has been put into the study of the vibrational behaviour and lattice dynamics of the major Earth-forming minerals (e.g. Kieffer, 1979*a*, *b*, *c*). In addition, attempts have been made to develop models which reproduce not only the vibrational behaviour of silicates but also their structural and physical properites (e.g. Devarajen and Funck 1974; Iishi, 1978). However, none of these previous efforts have been fully successful, and the quantitative link between the atomic forces which determine silicate structures and their vibrational and bulk properties has not been made. This shortcoming led McMillan (1985) to conclude that the lack of suitable models for the internal interactions in silicates represents one of the major obstacles to our achieving a full understanding of their macroscopic behaviour. In this paper we present results obtained from computer simulations of the lattice dynamics of the major mantle mineral forsterite (Mg_2SiO_4 olivine), in which, for the first time, the vibrational behaviour of a silicate is successfully predicted by using a model which describes the atomic interactions that determine the structural and elastic behaviour of that phase. The potentials used in this study were derived purely from the known structural and physical properties of simple oxides or silicates, and their ability to predict correctly the lattice dynamics of forsterite represents a fundamental advance over previous, force-constant models (e.g. Iishi, 1978), which were simply derived by fitting to the spectroscopic data that they aimed to model. The work described in this paper, therefore, establishes the previously elusive path between the microscopic or atomistic description of forsterite and its vibrational and hence thermodynamic behaviour.

The computer model adopted in this study of the lattice dynamics of forsterite uses an atomistic approach based upon the classical Born model of solids, in which potential functions represent the interactions between ions or atoms in the structure. It has been widely shown that this type of computer simulation may successfully predict both the structures of minerals and their elastic, dielectric and defect properties (e.g. Price and Parker, 1984; Price *et al.*, 1985; Catlow *et al.*, 1986). Early studies concentrated upon the use of pair-wise additive interatomic potentials, and ignored the role of many-body interactions. Recent successes, however, in modelling more complex silicates by using bond-bending terms to simulate some aspects of three-body interactions (Matsui and Busing, 1984; Sanders *et al.*, 1984; Catlow *et al.*, 1986) have provided the impetus for this study of forsterite, in which we have included O–Si–O bond-bending terms within our potential model to simulate the directional bonding thought to be important in silicate phases. In the following sections we describe in detail the potentials used in this study, and outline how they were used to calculate the Brillouin zone centre vibrational behaviour (infrared and Raman spectra) of forsterite. In subsequent sections, we compare the calculated vibrational behaviour of forsterite with its observed spectra, and discuss the significance of our model.

Atomistic simulation techniques

In principle, the bonding and related physical properties of any silicate can be studied by quantum mechanical methods, which directly describe the interactions of electrons and nuclei within a given system. However, because of the complexity of most silicates, such quantum mechanical studies are currently of limited utility. In contrast, the atomistic approach to modelling the behaviour of crystals is somewhat more simple and approximate, as it attempts only to describe the interactions between individual atoms or ions in the structure, rather than explicitly describing the interactions between each electron in the solid. This simplicity, however, allows the atomistic approach to be used to predict the physical and defect properties of crystals, while still providing useful insights into the nature of bonding within solids. In the atomistic approach, sets of interatomic potentials (usually assumed to be pair-wise additive) are developed to describe the effective net forces acting upon atoms within a structure. The forms of the model potentials used are designed to describe relatively simple, yet useful concepts of chemical bonding, such as ionic interactions, van der Waals bonding, and covalency (Born and Huang, 1954).

In ionic or semi-ionic solids such as silicates, it appears that the electrostatic or Coulombic energy terms, which result from the ionic charges of the atomic species, are the most important component of the cohesive energy. For an infinite, periodic array of atoms, the Coulombic energy can be written as

$$U_C = \sum_{ij} e^2 q_i q_j r_{ij}^{-1}, \qquad (1)$$

where e is the charge of the electron, q_i and q_j are the point charges associated with ions i and j, and r_{ij} is the distance between them. Ions are obviously not point charges, as assumed when calculating the Coulombic energy, but instead are composed of a nucleus and an associated electron cloud of finite size. It is necessary, therefore, to include a term in the potential which models the energetic effect of the overlap of the electron clouds, that results in a short-range repulsion which is most strongly felt by

nearest-neighbour ions. This short-range component of the two-body potential is well represented by the so-called Buckingham form

$$U_R = \sum_{ij} A_{ij} \exp(-r_{ij}/B_{ij}) - C_{ij} r_{ij}^{-6}, \quad (2)$$

where A_{ij}, B_{ij} and C_{ij} are parameters which must be derived for each pair-wise interaction.

For fully ionic, rigid-ion models, the above terms are generally the only components of the potential to be considered. However, it is well established that bonding in a silicate, such as olivine, is not expected to be fully ionic, and in particular a degree of directional, covalent bonding between silicon and its coordinating oxygens is to be expected. In recent studies of silicates two approaches have been used in an attempt to model this more complex type of bonding. Price and Parker (1984) used non-integral or partial ionic charges, either alone or with a Morse potential function to model the covalent Si–O bond. The Morse potential has the form

$$U_M = \sum_{ij} D_{ij} [1 - \exp\{E_{ij}(r_{ij} - r_O)\}]^2 - D_{ij}, \quad (3)$$

where D_{ij}, E_{ij} and r_O are parameters to be determined either empirically or from spectroscopic data. In contrast, Sanders *et al.* (1984) retained a fully ionic description of the charges, but modelled the directionality of the Si–O bond by introducing a bond-bending term into the potential, of the type

$$U_B = \sum_{ijk} k_{ijk}^B (\theta_{ijk} - \theta_O)^2, \quad (4)$$

where k_{ijk}^B is a derivable spring constant, θ_{ijk} is the O–Si–O bond angle, and θ_O is the tetrahedral angle. A similar approach to the problem of modelling the Si–O bond has been adopted with some considerable success by Matsui and co-workers (Matsui and Busing, 1984; Matsui and Matsumoto, 1985) in their elegant studies of beta-Mg_2SiO_4 and diopside. The inclusion of bond-bending terms into silicate potentials is a major development, as they appear successfully to model the effective three-body interactions and bond directionality that has long been recognized to play a significant role in determining the structure and properties of silicates.

In order to model the dielectric properties of a crystal correctly, it is often found to be necessary to develop a so-called shell model, as an alternative to the rigid-ion models so far described. A shell model provides a simple mechanical description of ionic polarizability, and its use is therefore essential if the defect and high-frequency dielectric behaviour of a material are to be studied. In this model, the atom or ion (it is frequently assumed that oxygen is the only polarizable atom in the structure) is described as having a core containing all the mass, surrounded by a massless shell of charge Y, representing the outer valence electron cloud. The core and shell are coupled by a harmonic spring, so that their interaction (U_S) can be described by the equation

$$U_S = \sum_i k_i^S r_i^2, \quad (5)$$

where k_i^S is the shell spring constant and r_i is the core–shell separation. In such a description the equation

$$\alpha_i = \sum_i (Ye)^2/(k_i^S + r_i), \quad (6)$$

describes the resulting polarizibility (α_i) of the ion i.

The derivable parameters of any potential may be determined empirically by using programs such as METAPOCS or WMIN (Catlow and Mackrodt, 1982; Busing, 1981), that fit the potential parameters to experimental data. Alternatively, they may be found by non-empirical methods, either by using Hartree–Fock molecular orbital calculations or by the computationally more economic electron gas methods, which are based on a statistical atom model (see Burnham, 1985). Once determined the interatomic potentials can be used with programs like METAPOCS to predict the structural, elastic and dielectric properties of a material. Normally, these perfect-lattice simulations are performed at an effective temperature of 0K, as they do not consider the vibrational energy of the system. However, in this investigation of forsterite, we have extended this usual approach to the study of perfect-lattice silicates to include the calculation of the normal modes of the lattice vibrations of olivine.

The relationship between the interatomic potential (U) and the normal modes of vibration of a structure has been described in detail in a variety of standard texts (e.g. Born and Huang, 1954; Ziman, 1964; Cochran, 1973). In brief however, the vibrations of atoms in a crystal consisting of N unit cells, each containing n atoms, can be described by $3nN$ Newtonian equations of motion. If U is the interatomic potential, then if any atom i in the crystal is displaced by an amount $\mathbf{u}_i$ from its equilibrium position, it will experience a restoring force F_i, where

$$F_i = \partial U / \partial \mathbf{u}_i. \quad (7)$$

Thus the equation of motion for each atom i, of mass m_i, can be expressed as

$$m_i \frac{\partial^2 u_i}{\partial t^2} = -\frac{\partial U}{\partial \mathbf{u}_i}. \quad (8)$$

From the theory of small displacements (e.g. Ziman, 1964) it can be shown that

$$\frac{\partial U}{\partial \mathbf{u}_i} = \sum_j \frac{\partial^2 U}{\partial \mathbf{u}_i \partial \mathbf{u}_j} \mathbf{u}_j \quad (9)$$

which can be interpreted as meaning that the sum on the right-hand side of equation (9) is the force acting on the i^{th} atom due to the displacement $\mathbf{u}_j$ of all the other j atoms in the crystal. In accordance with Block's theorem (e.g. Ziman, 1964) however, equations (8) and (9) must be translationally invariant, so we may write

$$\mathbf{u} = \mathbf{e}(\mathbf{q})\exp(i\mathbf{q}\cdot\mathbf{R} - w(\mathbf{q})t), \tag{10}$$

where $\mathbf{q}$ is the reciprocal lattice wave-vector for lattice waves, $w(\mathbf{q})$ is the frequency of the vibrational mode, $\mathbf{R}$ is the interatomic separation, and $\mathbf{e}(\mathbf{q})$ is the polarization vector describing the atomic displacements involved in the vibration. This treatment reduces the number of equations that now need to be considered from $3nN$ to $3n$, as the equivalence of all unit cells means that we need only consider one of them in order to calculate the dynamics of the whole assembly. Substitution of equations (9) and (10) into equation (8) yields

$$mw^2(\mathbf{q})\mathbf{e}(\mathbf{q}) = \mathsf{D}(\mathbf{q})\mathbf{e}(\mathbf{q}), \tag{11}$$

where $\mathsf{D}(\mathbf{q})$ is the dynamical matrix,

$$\mathsf{D}(\mathbf{q}) = \sum_{ij} \frac{\partial^2 U}{\partial u_i \partial u_j}\exp(i\mathbf{q}\cdot\mathbf{R}). \tag{12}$$

For a given value of $\mathbf{q}$, solution of equation (11) yields $3n$ eigenvalues which are the squared frequencies ($w^2(\mathbf{q})$) of each of the normal modes of the crystal, and $3n$ sets of eigenvectors ($\mathbf{e}_x(\mathbf{q})$, $\mathbf{e}_y(\mathbf{q})$ and $\mathbf{e}_z(\mathbf{q})$) which describe the pattern of atomic displacements for each normal mode.

In our study, we used the program CASCADE (Catlow and Mackrodt, 1982) which was written to solve such eigenvalue equations for a variety of potential forms. In the following sections we outline in greater detail the potentials used in our investigations, and present the eigenvalues and eigenvectors that these potentials predict for the normal modes of forsterite at values close to $\mathbf{q} = 0$, which correspond to the modes excited by the relatively long wavelength radiation used in infrared and Raman spectroscopy.

Potential models for forsterite

In this study of the lattice dynamics of forsterite we used the best examples of each of the three principle types of potential most commonly employed to model silicates, namely fully ionic pair-potential models, the partially ionic models, and potential models which include bond-bending terms (so called 'three-body potentials'). The fully ionic, pair-potential model used in this investigation was the potential P1 (Table 1), originally described by Price and Parker (1984). In this rigid-ion model, the values used for the short-range O–O interaction parameters were those originally derived by Catlow (1977) using Hartree–Fock methods. The Mg–O short-range term used was that derived by Lewis (1985) by fitting to the structural and elastic data of MgO, while the Si–O interaction term was obtained by fitting the potential to the observed structural data of forsterite. This potential was, therefore, largely developed on the assumption that potential parameters are transferable from one structure to another. In contrast, the partially ionic potentials P3 and P4 (Price and Parker, 1984) used in this investigation were derived purely empirically. The potential P3 was obtained using the program WMIN (Busing, 1981) to optimise the ionic charges and short-range terms with respect to the structural data of olivine. The potential P4 was similarly derived, however it also included a Morse function intended to model the local effect of Si–O covalent bonding.

Table 1. Parameters of potentials used to model forsterite

		P1	P3	P4	THB1
q_{Mg}		+2.0	+1.6	+1.726	+2.0
q_{Si}		+4.0	+2.0	+1.380	+4.0
q_O		-2.0	-1.3	-1.208	-2.848*
A_{Mg-O}	eV	1428.5	13991.0	2269.7	1428.5
A_{Si-O}	eV	473.2	4170.8	734.7	1283.9
A_{O-O}	eV	22764.3	1.36×10^{10}	9.27×10^{8}	22764.3
B_{Mg-O}	Å	0.2945	0.2005	0.2537	0.2945
B_{Si-O}	Å	0.4157	0.2000	0.2274	0.3205
B_{O-O}	Å	0.1490	0.1010	0.1136	0.1490
C_{O-O}	$eVÅ^6$	60.08	-	-	27.88
C_{Si-O}	$eVÅ^6$	-	-	-	10.66
D_{Si-O}	eV	-	-	4.46	-
E_{Si-O}		-	-	1.97	-
k^S	$eVÅ^{-2}$	-	-	-	74.92
k^B	$eVrad^{-2}$	-	-	-	2.09

*This is the shell charge. The oxygen core charge used was +0.848.

The three-body potential, THB1, considered in this investigation was constructed using the same philosophy of potential transferability that was adopted in the development of potential P1. The same O–O and Mg–O short-range repulsion terms were used in the THB1 potential as were used in potential P1. The Si–O short-range parameters and the O–Si–O bond-bending spring constant, however, were taken from Sanders *et al.* (1984), who derived these terms by fitting them to the structural and elastic properties of quartz. In addition to a bond-bending term, the quartz potential of Sanders *et al.* (1984) included a shell model potential to describe the oxygen polarizability; this

feature was also incorporated into the potential THB1.

Details of how successful potentials P1, P3 and P4 are in describing the structural and elastic behaviour of forsterite are discussed in detail by Price and Parker (1984). However, in brief, all of these potentials satisfactorily reproduce the observed forsterite cell parameters to within *c.*1·5%, and represent the best potentials so far developed to describe the elastic behaviour of forsterite, predicting bulk (K) and shear (μ) moduli of 1.25–1.41 Mbars and 0.79–1.0 Mbars respectively, which compare favourably with the experimentally determined values of 1.25 and 0.81 Mbars. It is most encouraging and impressive that the potential THB1, derived purely by fitting to the properties of binary oxides, is as successful at predicting the structural, elastic and dielectric (ε_0 and ε_∞) constants of the ternary oxide forsterite as the empirically derived potentials P3 and P4. The predicted forsterite cell parameters (Table 2) are accurate to within 1%, and the agreement between the observed and calculated elastic constants is highly satisfactory, with predicted bulk and shear moduli of 1.38 and 0.97 Mbars respectively.

It was pointed out by Price and Parker (1984) that the accurate prediction of the lattice parameters and the elastic properties of a crystal provided a stringent test of any potential model, since they required the accurate modelling of both the first and second derivatives of the potential function. As discussed above, the vibrational behaviour of a crystal is also dependent upon the second derivative of the interatomic potential. Consequently, we had confidence that these potentials (P1, P3, P4 and THB1) would reproduce the major features of the lattice vibrational behaviour of forsterite. The extent to which these expectations were fulfilled is outlined in the following section.

The symmetry and frequencies of the q = 0 lattice vibrations of forsterite

Forsterite has four formula units, and consequently 28 atoms per unit cell, which give rise to 84 normal modes of vibration. Detailed analysis of the symmetry of these modes has been presented in a variety of works (see McMillan, 1985), but in brief the sum of the irreducible representation of the forsterite space group (*Pbnm*) can be written as

$$\Gamma^{\text{total}} = 11A_g + 11B_{1g} + 7B_{2g} + 7B_{3g} + 10A_u + 10B_{1u} + 14B_{2u} + 14B_{3u}. \quad (13)$$

At the centre of the Brillouin zone ($\mathbf{q} = 0$), three of these 84 modes are purely translational;

$$\Gamma^{\text{trans}} = B_{1u} + B_{2u} + B_{3u}. \quad (14)$$

The remaining 81 modes, however, are truly vibrational in nature. Of these, those which are symmetric with respect to inversion (grade or g) are Raman active, 10 with A_u symmetry are spectroscopically inactive, and the remaining 35 modes with B_{1u}, B_{2u} and B_{3u} symmetry are infrared active.

Table 2. The structural and physical properties of forsterite predicted by potential THB1.

		Observed	THB1
a	Å	4.754	4.784
b	Å	10.194	10.261
c	Å	5.981	5.991
K	Mbar	1.25	1.38
μ	Mbar	0.81	0.97
ε_0		7.32	6.50
ε_∞		2.72	2.10

The infrared and Raman spectra of forsterite have been extensively studied (e.g. Servoin and Piriou, 1973; Paques-Ledent and Tarte, 1973; Iishi, 1978), and there is general agreement on the frequencies of the characteristic vibrations (Table 3). Most infrared and Raman bands have been unambiguously identified, but there is still some controversy over some of the weaker or more poorly resolved peaks (see McMillan, 1985). The spectroscopically active vibrational modes have frequencies that lie in the range between 1100 cm^{-1} and 150 cm^{-1}, but modes with frequencies greater than 800 cm^{-1} are clearly separated by a 150 cm^{-1} wide gap from those with frequencies below *c.*650 cm^{-1}. It is generally agreed that the high frequency modes are the result of Si–O stretching motions, while modes with frequencies below 650 cm^{-1} are thought to be the result of vibrations involving more complex displacements of Si, O and Mg. Considerable uncertainty remains, however, concerning the detailed nature of the atomic motions in many vibrational modes, despite the efforts which have been made to elucidate them by using isotopic substitution techniques (e.g. Paques-Ledent and Tarte, 1973). This aspect of the lattice dynamics of forsterite will be discussed in greater detail in the following section.

In addition to these experimental studies, attempts have been made to model empirically the lattice dynamics of forsterite. These studies by Devarajan and Funck (1974) and by Iishi (1978) involved the development of force-constant models to describe the vibrational behaviour of Mg_2SiO_4. In such an approach, interactions between atoms are described by a simple harmonic spring constant, and occasionally include Coulombic effects. The numerical values of the spring constants are

Table 3. Observed and calculated $\underline{q}=0$ vibration frequencies of forsterite.

	Obs^	P1	P3	THB1	I	DF
RAMAN ACTIVE MODES						
Ag	960-966	926*	1022*	943	962	962
	854-856	788*	850	851	886	867
	822-826	729*	777*	807	839	827
	606-609	603	650*	630	606	625
	541-545	471*	583*	580*	537	556
	420-424	383*	462*	427	430	435
	334-340	347	403*	360	350	347
	325-329	318	386*	344	318	329
	304-305	306	342*	312	269*	289
	221-227	233	208	221	213	208
	181-183	170	197	184	165	167
B1g	972-976	1080*	1066*	963	962	965
	863-866	875	850	864	888	870
	835-839	842	777*	821	839	826
	626-632	664	705*	667	616	626
	577-583	476*	642*	617*	519*	526*
	428-434	427	471*	454	418	423
	418 +	409	429	428	394	379*
	314-318	344	401*	337	333	334
	260-265+	306*	350*	325*	287	294
	215-224	262*	276*	269*	217	231
	149-192+	212	229*	231*	206	192
B2g	880-884	965*	816*	901	894	887
	583-588	528*	680*	611	563	570
	436-441	464	476*	433	467	457
	354-368	378	434*	365	373	383
	324 +	335	374*	345	312	306
	237-244	224	238	207	268	276*
	142-150	175	168	149	157	153
B3g	917-922	1048*	798*	960*	894	893
	588-595	580	742*	606	548*	556*
	407-412	400	463*	417	424	426
	371-376	368	437*	390	362	351
	312-318	335	355*	327	323	334
	272 +	272	267	250	269	276
	226 +	116*	188*	133*	242	240
INACTIVE MODE						
Au	.	793	814	938	.	890
	.	553	563	519	.	552
	.	476	544	479	.	496
	.	437	494	452	.	435
	.	374	424	391	.	397
	.	325	383	340	.	346
	.	285	317	271	.	262
	.	256	270	250	.	233
	.	174	168	166	.	178
	.	8	96	58	.	112

	Obs^	P1	P3	THB1	I	DF
INFRARED ACTIVE MODES						
	TO-LO	TO-LO	TO-LO	TO-LO	TO-LO	
B1u	885-994	630-631*	780-781*	879-1028	893-903	884
	502-585	551-552	560-568	513-598	512-512*	544
	483-489	504-505	536-546*	476-502	482-494	508
	423-459	435-437	455-458	450-475	439-444	456
	365-371	427-435*	446-455*	375-390	391-391	404*
	296-318	350-374*	352-353*	347-362*	336-350*	366*
	274-278	319-319*	348-349*	313-321*	240-244*	237*
	224 +	278-279*	315-316*	250-251	209-209	229
	201 +	158-159*	198-199	176-177	185-186	170*
B2u	987-993	872-873*	1026-1027*	995-1008	958-959*	958
	882-979	829-830*	834-842*	874-980	900-906*	863
	838-843	717-750*	791-826*	815-817	834-834	825
	.....	669-672	657-658	671-672		622
	537-597	654-651*	548-550	558-605	581-581	559
	510-516	500-514	519-524	538-547	542-543	507
	465-493	483-484	509-511	488-524	467-479	450
	421-446	439-445	467-483	448-488	427-430	418
	400-412	390-398	458-488*	431-444	364-364*	355*
	352-376	329-350	394-403	355-390	338-354	333
	294-313	275-277	327-344*	298-308	280-284	265
	280-283	234-244*	323-324*	265-290	250-250*	
	244 +					219
	144 +	147-148	151-152	146-146	137-138	128
B3u	980-1086	1246-1261*	1014-1015	995-1084	957-967*	954
	957-963	1169-1170*	898-985*	960-991	901-901*	873*
	838-845	794-824	853-873	812-815	832-835	823
	601-645	697-708*	744-760*	657-658	569-577*	617
	562-566	565-623	667-679*	573-638*	529-528*	545
	498-544	553-554	579-608*	520-571	473-473*	503
	438-469	512-514*	531-536*	482-516*		448
	403-438	436-439	485-509*	437-471*	421-421	434
	378-386	413-427	466-467*	376-394	359-376	342*
	320-323	347-368	365-366*	349-349	327-332	312
	293-298	288-304	320-322	307-313	280-280	
	274-276	259-260	295-296	293-293	242-241*	259
	224 +				218-219	212
	201 +	184-185	198-199	193-197	190-191	189

^ Range of observed values taken from Devarajan and Funck(1975), Iishi (1978) and Servoin and Piriou (1973). The frequencies chosen do not include those now thought to be the result of the leakage of strong LO modes of one symmetry into spectra of another (Piriou and McMillan, 1983).
+ Weak bands, or those infrquently experimentally determined.
* Calculated frequencies which are in error by more than 30 wavenumbers.

determined purely by fitting to the observed vibrational frequencies, and are therefore in no way predictive. Neither are they able to be used in other atomistic studies, such as point defect or diffusion modelling. Devarajan and Funck (1974) fitted 24 parameters to 62 observed vibrational frequencies, while Iishi (1978) developed models with up to 14 parameters fitted to forsterite spectra. The success and accuracy of these fitting exercises can be determined by inspection of Table 3. Devarajan and Funck (1974) calculated frequencies (column DF in Table 3) that are in excellent accord with their set of observed values, with only 11 frequences in error by more than 30 cm^{-1}. Their model included no Coulombic effects, so that they were not able to reproduce the TO-LO splitting of the infrared active modes. In contrast, Iishi's (1978) most successful model did contain a Coulombic component, but as it has fewer overall parameters than that of Devarajan and Funck (1974) it is not surprising that the fit that Iishi achieved with his model is slightly inferior to that of Devarajan and Funck. Nevertheless, of the calculated values obtained by Iishi (column I in Table 3) only 16 are in error by more than 30 cm^{-1}. It should be noted, however, that there are some minor differences between the sets of frequencies used by these workers in deriving their force-constant models, which makes it difficult to compare them directly.

The detailed experimental and theoretical studies that have already been performed on forsterite make it, therefore, an ideal material to be used to test the strengths and weaknesses of the recently developed atomistic models of silicates. In Table 3, we present the vibrational frequencies of the normal modes of forsterite predicted by three of the potential models considered in this study. The two-body potentials P1 and P3 predict vibrational frequencies which are in poor overall agreement with those observed experimentally. Typically the predicted and observed frequencies differ by 40–60 cm^{-1}, and significantly the gap in the vibrational spectra between 800 and 650 cm^{-1}, characteristic of forsterite, is not reproduced. It was found that the partially ionic potential P4 gave even worse predicted frequencies than did P1 and P3. In particular, the predicted Si–O stretching frequencies were up to 1000 cm^{-1} too large, and the overall

agreement was so poor as not to merit inclusion in Table 3. In contrast, however, the potential THB1, derived purely from MgO (periclase) and SiO_2 (quartz), predicts vibrational frequencies for forsterite which are in excellent agreement with those observed, and have accuracies which compare favourably with those achieved by the models of Devarajan and Funck (1974) and Iishi (1978). Of the 71 infrared and Raman active vibrational modes predicted by the THB1 potential, 61 had frequencies within 30 cm^{-1} of unambiguously observed modes, and only 4 were in error by more than 50 cm^{-1}. There appears to be some experimental uncertainty over the exact frequencies of some of the infrared active modes, which makes the exact quality of the prediction of these modes difficult to assess. More detailed experimental studies are required to resolve these problems. The average error in the predicted Raman frequencies is only 20 cm^{-1}, and the predicted magnitudes of the TO–LO splittings of the infrared active modes are generally comparable with those observed, in contrast to those calculated by Iishi (1978). Currently, there is no way to assess the accuracy of the predicted frequencies of the 10 spectroscopically inactive A_u modes, however it appears that the values predicted by the potential THB1 and those calculated by Devarajan and Funck (1974) are broadly in agreement.

As was suggested above, it appears that the prediction of vibrational frequencies provides a most stringent test of any silicate potential. Although potentials P1, P3 and P4 all adequately reproduce the structural and elastic properties of forsterite, they fail to predict its vibrational behaviour correctly. It appears that these potentials are particularly poor in modelling the interactions between Si and O, as potentials P1 and P3 do not predict the 650–800 cm^{-1} frequency gap between Si–O stretching modes and other lower frequency modes, and potential P4 predicts unreasonably high Si–O stretching frequencies. It must be concluded, therefore, that Si–O interactions play a relatively insignificant role in determining the structural and elastic properties of forsterite, and that inadequacies in those parts of the potential that describe their interaction are only revealed in attempts to calculate their vibrational behaviour. The success of the potential THB1 in correctly predicting the vibrational frequencies of forsterite suggests that the O–Si–O bond bending term, unique to this potential, reflects a major and significant feature of Si–O bonding, and that any future modelling of silicates must take into account the directionality of the Si–O bond.

We conclude, therefore, that of all the potentials considered only THB1 satisfactorily reproduces the vibrational behaviour of forsterite, and that despite having been derived from MgO and SiO_2, it is at least as successful in predicting the frequencies of the normal vibrational modes of forsterite as are the force-constant models obtained by fitting to its vibrational spectra. In the next section we consider in more detail some of the outstanding problems of the lattice dynamics of forsterite, and assess how the predictions made by the potential THB1 can be used to resolve some of these ambiguities.

The crystal dynamics of forsterite

As discussed in the previous section, the frequencies of both the infrared and Raman spectra of forsterite are relatively well known. In contrast however, the actual vibrations or atomic displacements which give rise to the adsorption bands in these spectra of forsterite are far less well determined. It was briefly mentioned that the general principles of spectroscopy and studies of molecular vibrational spectra have led to the deduction that the high frequency bands (1100–800 cm^{-1}) are the result of Si–O stretching motions. Indeed, the interpretation of the general vibrational behaviour of forsterite can be greatly simplified by considering, in the first instance, the constituent SiO_4 groups to be dynamically isolated. Under these circumstances, it would be expected that the higher frequency vibrational modes in forsterite would be associated with internal vibrations within the SiO_4 tetrahedron, while the lower frequency modes would be the result of external or lattice vibrations, involving rotation or libration of the SiO_4 tetrahedra as well as the translation of the SiO_4 group and the Mg cations. It should be noted, however, that both the classification of crystal vibrations as internal or external, and the subdivision of these latter into rotational and translational vibrations should be viewed with considerable caution. In the general case, lattice vibrations are not purely translational or rotational, and the separation of internal vibrations from lattice vibrations is only approximate, even in molecular crystals (Lazarev, 1974). Nevertheless, as will be shown below, significant progress towards understanding the lattice dynamics of forsterite can be made if this simple view of its vibrational behaviour is adopted.

An isolated tetrahedral molecule is known to have four distinct vibrational modes. The higher frequency modes involve symmetric (ν_1) and anti-symmetric (ν_3) stretching, while the symmetric (ν_2) and anti-symmetric (ν_4) bending modes are generally of lower frequency (Fig. 1). Conventional symmetry analysis (e.g. McMillan, 1985) has shown that the simple ν_1 and ν_3 modes of the isolated tetrahedron would give rise to 15 active modes in forsterite,

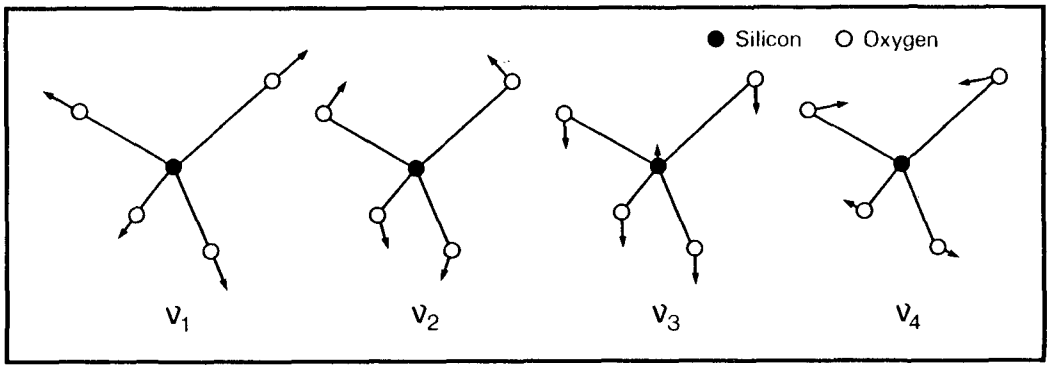

FIG. 1. The four independent vibrational modes of an isolated tetrahedral molecule.

which correspond exactly to the number of bands identified in the high frequency (1100–800 cm^{-1}) region of its infrared and Raman spectra. The inference that these high frequency modes are essentially due to internal Si–O stretching is supported by the unpolarised infrared and Raman studies performed by Paques-Ledent and Tarte (1973) on forsterites containing varying $^{28}Si/^{30}Si$ and $^{24}Mg/^{26}Mg$ isotope ratios. These workers noted that bands in the range 1100–800 cm^{-1} were unaffected by the Mg isotope content, indicating that little or no Mg translations were involved in these high frequency modes. They found, however, that bands in the range 991 cm^{-1}, 960–950 cm^{-1} and 900–885 cm^{-1} were sensitive to variations in the Si isotope content, and inferred that they were related to ν_3, anti-symmetric stretching modes, in which significant Si displacement is to be expected.

Paques-Ledent and Tarte (1973) also found that bands in the range 650–475 cm^{-1} showed a frequency dependence on both Si and Mg isotope content. They were unable to infer the exact nature of the vibrations involved, however it is generally accepted that the vibrations in this region of the forsterite spectra are associated with internal Si–O bending vibrations. Obviously, from the observations of Paques-Ledent and Tarte (1973), these vibrations must be of significantly mixed nature. Below 475 cm^{-1}, these workers found infrared peaks at 466, 425, 415, 364, 320, 300 and 277 cm^{-1} which showed large frequency shifts with Mg isotope variation, but which had little Si frequency dependence (McMillan, 1985). From there observations Paques-Ledent and Tarte (1973) inferred that the bands were associated with large Mg translations and possibly SiO_4 rotations. All the remaining bands observed in their study appeared to involve both Mg and Si displacements.

Various other experimental investigations have been performed (see McMillan, 1985) in an attempt to elucidate the general features of the atomic motions involved in the vibrations which give rise to the infrared and Raman spectra of forsterite. However, by themselves such studies will be incapable of describing the detailed nature of the atomic motions associated with each vibrational mode, since these exact considerations can only be obtained from atomistic models of the lattice dynamics of forsterite. As described above, the solution of equation (11) yields not only the eigenvalues of each of the normal modes, from which the frequencies of the vibrations are derived, but also the eigenvectors which describe the pattern and relative magnitude of the atomic displacements for each mode. In their studies, Devarajan and Funck (1974) and Iishi (1978) evaluated the eigenvectors which resulted from their force-constant models, and presented their tentative assignments for the vibrational modes of forsterite. In general, their assignments were in accord with those inferred experimentally. However, as pointed out by McMillan (1985) the models of Iishi and of Devarajan and Funck were themselves fitted to a specific interpretation of the forsterite spectra, and consequently it is not surprising that they produce results in broad agreement with those from which they started.

In Fig. 2, we present projections of the forsterite structure on to which are plotted the eigenvectors calculated using potential THB1 for each of the forsterite normal modes. In Table 4 we have attempted to summarise the dominant vibrational components in each of these modes, in terms of the internal vibrations of a SiO_4 tetrahedron (ν_1, ν_2, ν_3 and ν_4), SiO_4 group rotations (R) about the x, y and z crystallographic axes, and of translations (T) of the SiO_4 group and Mg1 (at the centre of symmetry) and Mg2 (on the mirror plane) cations parallel to

the x, y or z axes. Detailed study of Fig. 2 shows that most of the modes involve complex patterns of atomic motion, and therefore exhibit evidence of considerable mixing of the various simple modes discussed above. As a result, Table 4 should be viewed only as an approximate description of the forsterite lattice vibrations. However, we can conclude that the general features of the lattice dynamics of forsterite, which are predicted by potential THB1, are in excellent agreement with those previously inferred from experiment. Fig. 2 and Table 4 show that the high frequency vibrations (1100–800 cm^{-1}) are predicted only to involve SiO_4 internal ν_1 and ν_3 modes, while the bands in the range 650–400 cm^{-1} are largely due to ν_2 and ν_4 Si–O stretching modes but also involve significant Si and Mg displacements, as suggested by the isotopic studies of Paques-Ledent and Tarte (1973). Bands with frequencies below *c.*400 cm^{-1} are predicted to be external modes of generally mixed character.

Table 4. Assignments of the vibrational modes predicted by potential THB1

Ag	943	ν_3	B1g	963	ν_3
	851	ν_3		864	ν_3
	807	ν_1 + Ty(Si)		821	ν_1 + Txy(Si)
	630	ν_4 + Tx(Si)		667	ν_4 + Tx(Si) + Ty(Mg)
	580	ν_4 + Ty(Si,Mg2)		617	ν_4 + Ty(Si) + Ty(Mg)
	427	ν_2 + Txy(Si,Mg2)		454	ν_2 + Tx(Mg2)
	360	Rz(SiO_4) + Txy(Mg2)		428	Rz(SiO_4) + Ty(Mg2)
	344	Rz(SiO_4) + Txy(Mg2)		337	Rz(SiO_4) + Tx(Mg2)
	312	Ty(SiO_4,Mg2)		325	Rz(SiO_4) + Txy(Mg2)
	221	Ty(SiO_4,Mg2)		269	Txy(SiO_4,Mg2)
	184	Rz(SiO_4) + Tx(Mg2)		231	Ty(SiO_4) + Tx(Mg2)
B2g	901	ν_3	B3g	960	ν_3 + Tz(Mg2)
	611	ν_4 + Tz(Si)		606	ν_4 + Tz(Si,Mg2)
	433	ν_2		417	ν_2 + Tz(Si)
	365	Ry(SiO_4) + Tz(Mg2)		390	Ry(SiO_4) + Tz(Mg2)
	345	Tz(SiO_4,Mg2)		327	Tz(SiO_4,Mg2)
	207	Rx(SiO_4) + Tz(Mg2)		250	Rx(SiO_4) + Tz(Si,Mg2)
	149	Rx(SiO_4) + Tz(Mg2)		133	Rx(SiO_4) + Tz(Si,Mg2)
Au	938	ν_3	B1u	879	ν_3
	519	ν_4 + Tz(Si,Mg2)		513	ν_4 + Tz(Si)
	479	ν_2 + Tz(Si)		476	ν_2 + Tz(Si)
	452	Txyz(Mg1) + Tz(SiO_4,Mg2)		450	Txyz(Mg1) + Ry(SiO_4)
	391	Ry(SiO_4) + Tz(Mg2) + Tx(Mg1)		375	Tx(Mg1) + Ry(SiO_4)
	340	Txyz(Mg1) + Ry(SiO_4)		347	Txy(Mg1) + Rx(SiO_4) + Tz(Mg2)
	271	Txz(Mg1) + Rx(SiO_4)		313	Txyz(Mg1) + Rx(SiO_4) + Tz(Mg2)
	250	Txyz(Mg1) + Rx(SiO_4) + Tz(Mg2)		250	Rx(SiO_4)
	166	Ty(Mg1) + Rx(SiO_4)		176	Ty(Mg1)
	58	Txyz(M1) + Tz(SiO_4,Mg2)		0	Tz(Mg1,SiO_4,Mg2)
B2u	995	ν_3	B3u	1084	ν_3
	874	ν_3		991	ν_3
	815	ν_1 + Txy(Si)		815	ν_1
	671	ν_4 + Tz(Mg1,Si,Mg2)		658	ν_4 + Tx(Si)
	558	ν_4 + Ty(Mg1,Si,Mg2)		638	ν_4 + Tx(Mg1,Si,Mg2)
	538	ν_2 + Tz(Mg1)		571	ν_2 + Txy(Mg1,Si,Mg2)
	488	ν_2 + Txyz(Mg1)		516	Tyz(Mg1) + Ty(SiO_4,Mg2)
	448	Tx(Mg1) + Rz(SiO_4)		471	ν_2 + Tz(Mg1)
	431	Txz(Mg1) + Rz(SiO_4)		394	Rz(SiO_4) + Txy(Mg2)
	355	Ty(Mg2) + Rz(SiO_4)		350	Txyz(Mg1) + Ty(SiO_4,Mg2)
	298	Ty(Mg1,SiO_4) + Tx(Mg2)		313	Tx(Mg2) + Rz(SiO_4) + Txy(Mg1)
	265	Ty(Mg1) + Rz(SiO_4) + Tx(Mg2)		293	Ty(Mg1,SiO_4,Mg2)
	146	Tx(Mg1,SiO_4)		193	Ty(Mg1,SiO_4)
	0	Ty(Mg1,SiO_4,Mg2)		0	Tx(Mg1,SiO_4,Mg2)

Some of the more detailed predictions made by the potential THB1, support the inferences drawn from previous experimental studies carried out into the lattice dynamics of forsterite. Thus for example, as discussed by McMillan (1985), significant effort has been expended in determining which bands in the A_g and B_{1g} Raman spectra of forsterite correspond to ν_1 stretching modes and which to ν_3-like modes. The isotopic studies of PaquesLedent and Tarte (1973) showed that all of the high frequency A_g and B_{1g} Raman modes had frequencies which were dependent upon the Si isotope content, and concluded that some mixing of ν_1 and ν_3 modes must occur. The prediction of the potential THB1 are in full agreement with this conclusion, and show that the modes which are dominantly ν_1 in character also have a significant Si displacement. We would suggest that the band with most ν_1 character has a lower frequency than the largely ν_3-like mode. This is in conflict, however, with the suggestion made by Piriou and McMillan (1983), who propose that the ν_1-like band may be of higher frequency than the lowest frequency ν_3 band. At lower frequencies, we find that the potential THB1 predicts that there are eleven infrared bands (Table 4) in which there is little or no Si translation. The frequencies of these bands are 488, 450, 448, 431, 375, 313, 307, 265, 250 and 176 cm^{-1} and appear to be a good match for those bands found by Paques-Ledent and Tarte (1973) to have frequencies independent of Si isotope content at 466, 425, 415, 364, 320, 300 and 277 cm^{-1} (McMillan, 1985). It appears, therefore, that the potential THB1 not only reproduces the general features of the lattice dynamics of forsterite, but also models the majority of the known specific aspects of its behaviour. Consequently, we feel that although it is not possible to test all of the predictions made using potential THB1 concerning the details of the atomic vibrations that occur in forsterite, and which are shown in Fig. 2, it is highly probable that they are essentially correct.

Conclusion

In potential THB1, we have a model of the effective interatomic interactions in forsterite that is of sufficient accuracy as to reproduce not only the major structural features of forsterite, but also to predict its lattice dynamics as successfully as any previously developed model. This capability is made even more impressive when it is recalled that the empirically derived parts of the potential were obtained purely by fitting to the structural and physical properties of MgO and SiO_2, and that they contain no input derived from a previous knowledge of the behaviour of forsterite. Its success is a powerful testimony to the philosophy of potential transferability, which holds that if a potential is presented as being able to describe the real nature of effective interatomic interactions within a solid, then it should be transferable from one structure

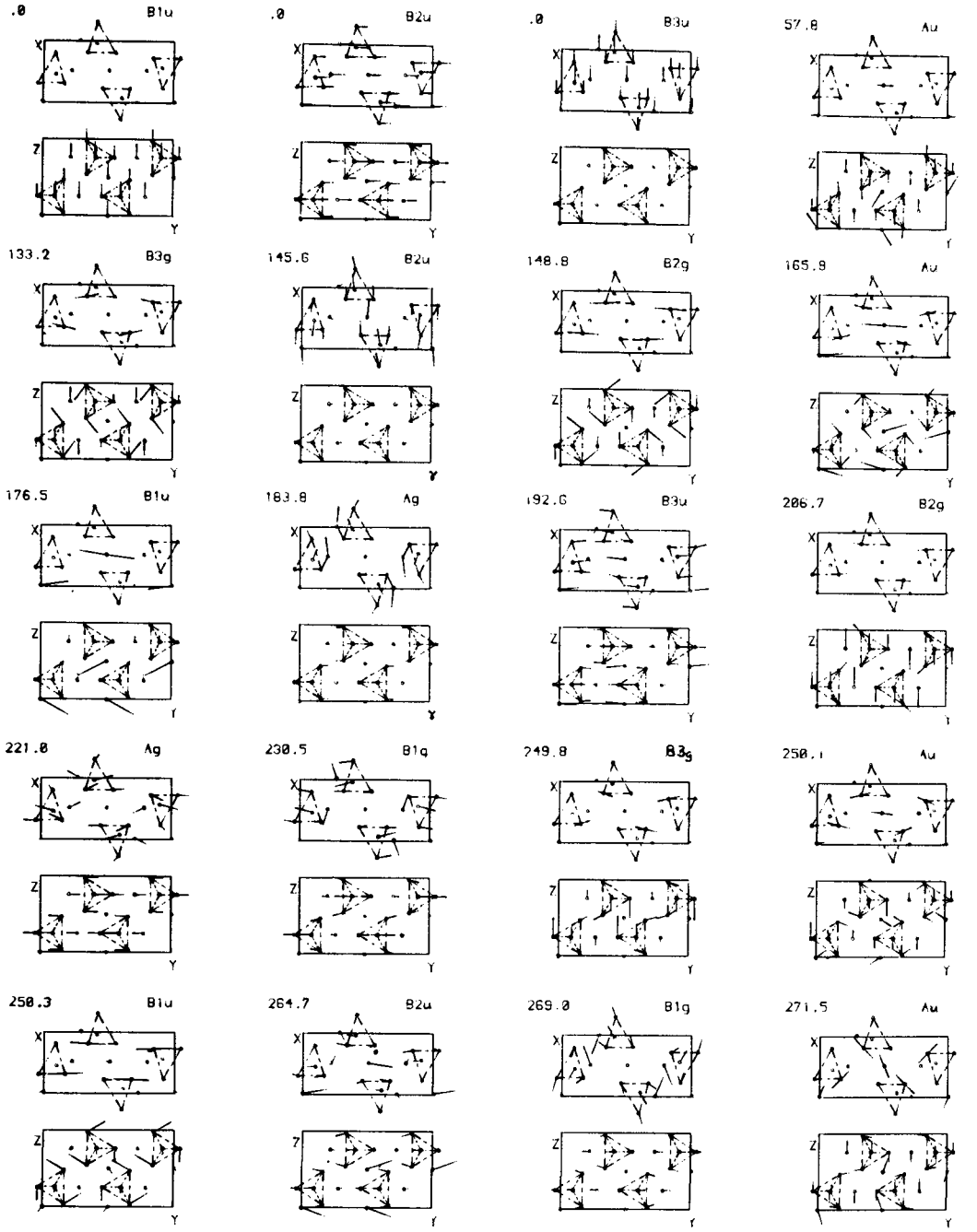

FIG. 2. The 84 vibrational modes of forsterite predicted by potential THB1. The modes shown are those calculated for a phonon wave-vector of $\mathbf{q} = (0.0, 0.0, 0.001)$.

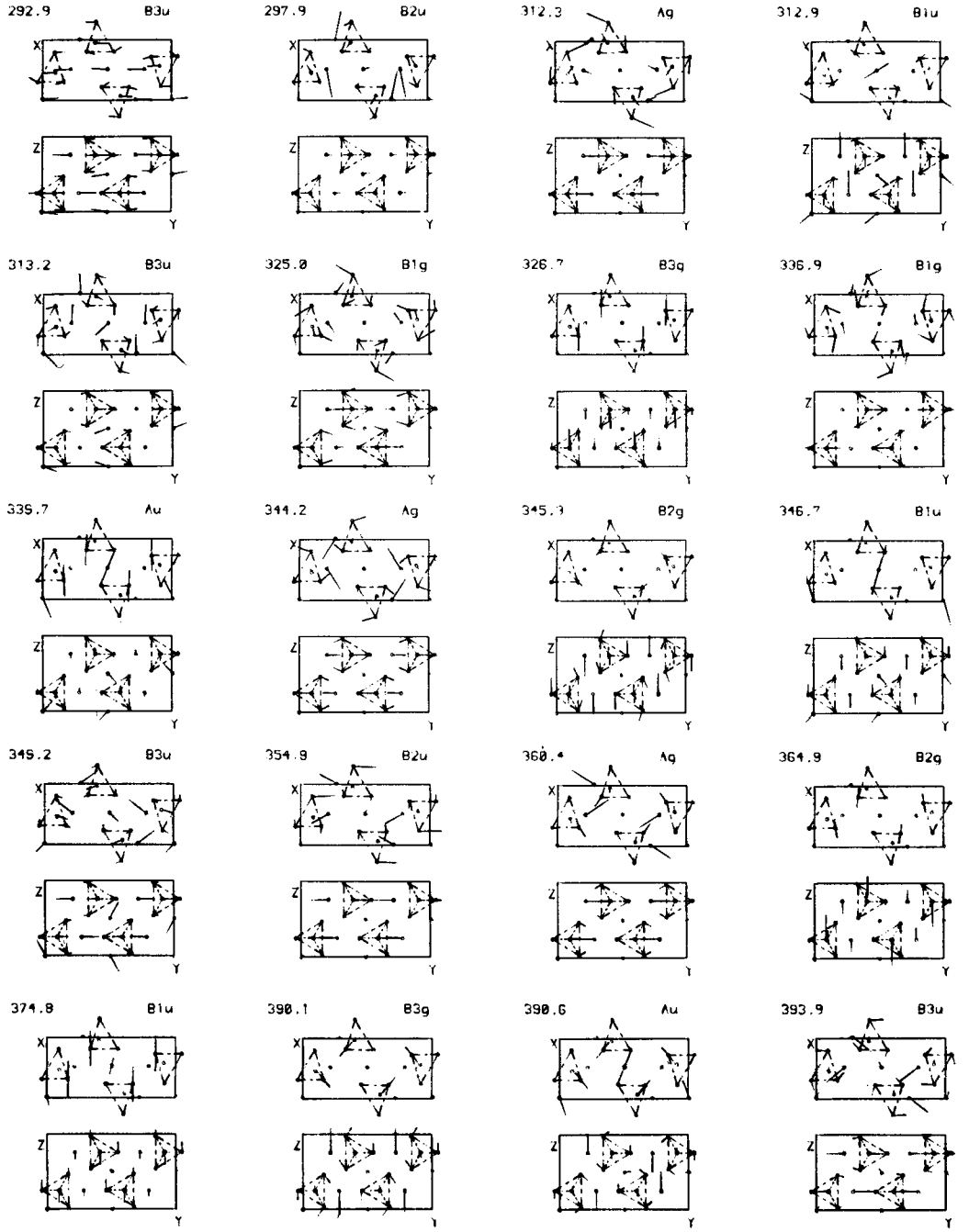
292.9 B3u
297.9 B2u
312.3 Ag
312.9 B1u
313.2 B3u
325.0 B1g
326.7 B3g
336.9 B1g
339.7 Au
344.2 Ag
345.3 B2g
346.7 B1u
348.2 B3u
354.9 B2u
360.4 Ag
364.9 B2g
374.8 B1u
390.1 B3g
390.6 Au
393.9 B3u

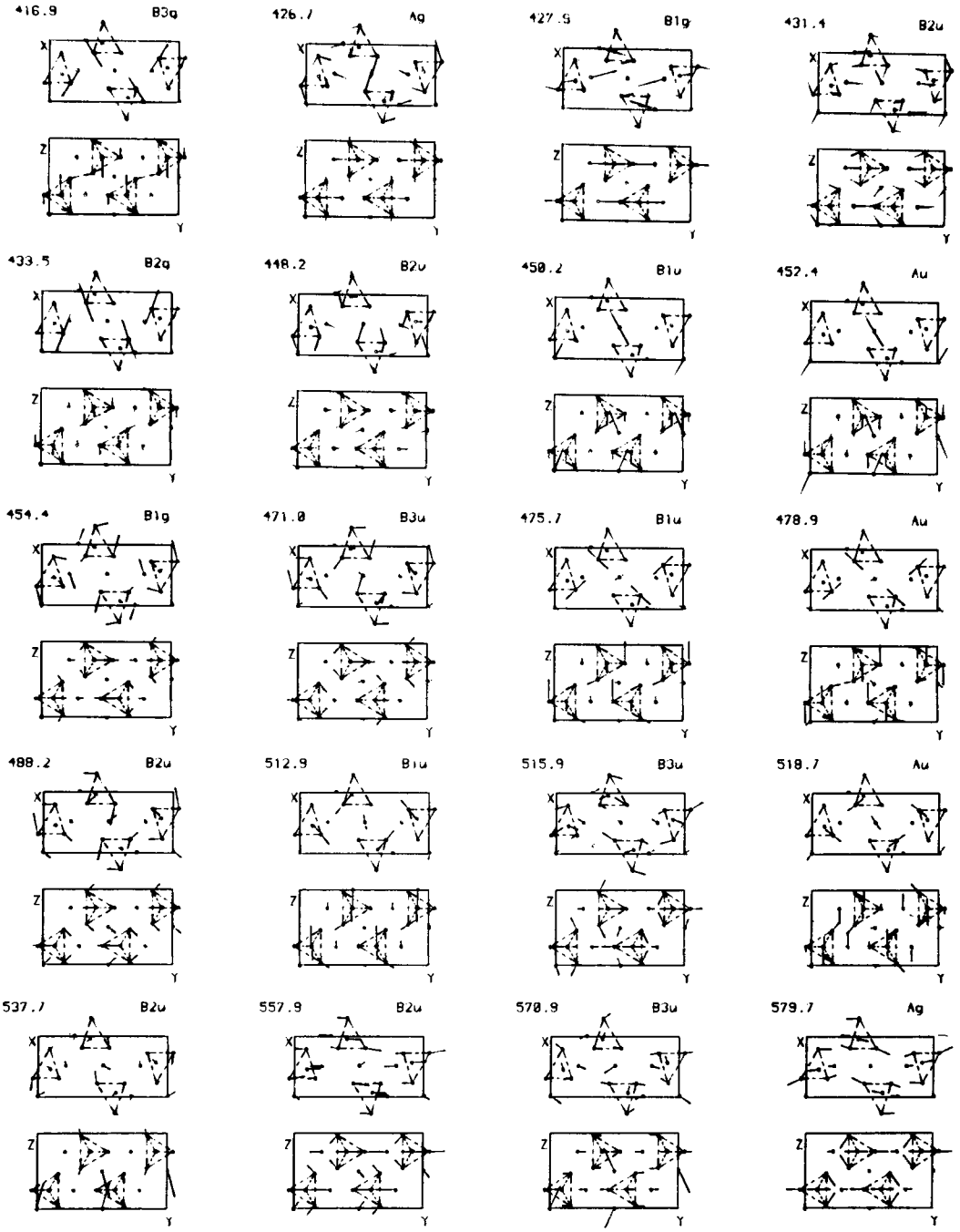
416.9 B3g
426.7 Ag
427.9 B1g
431.4 B2u
433.5 B2g
448.2 B2u
450.2 B1u
452.4 Au
454.4 B1g
471.0 B3u
475.7 B1u
478.9 Au
488.2 B2u
512.9 B1u
515.9 B3u
518.7 Au
537.7 B2u
557.9 B2u
570.9 B3u
579.7 Ag

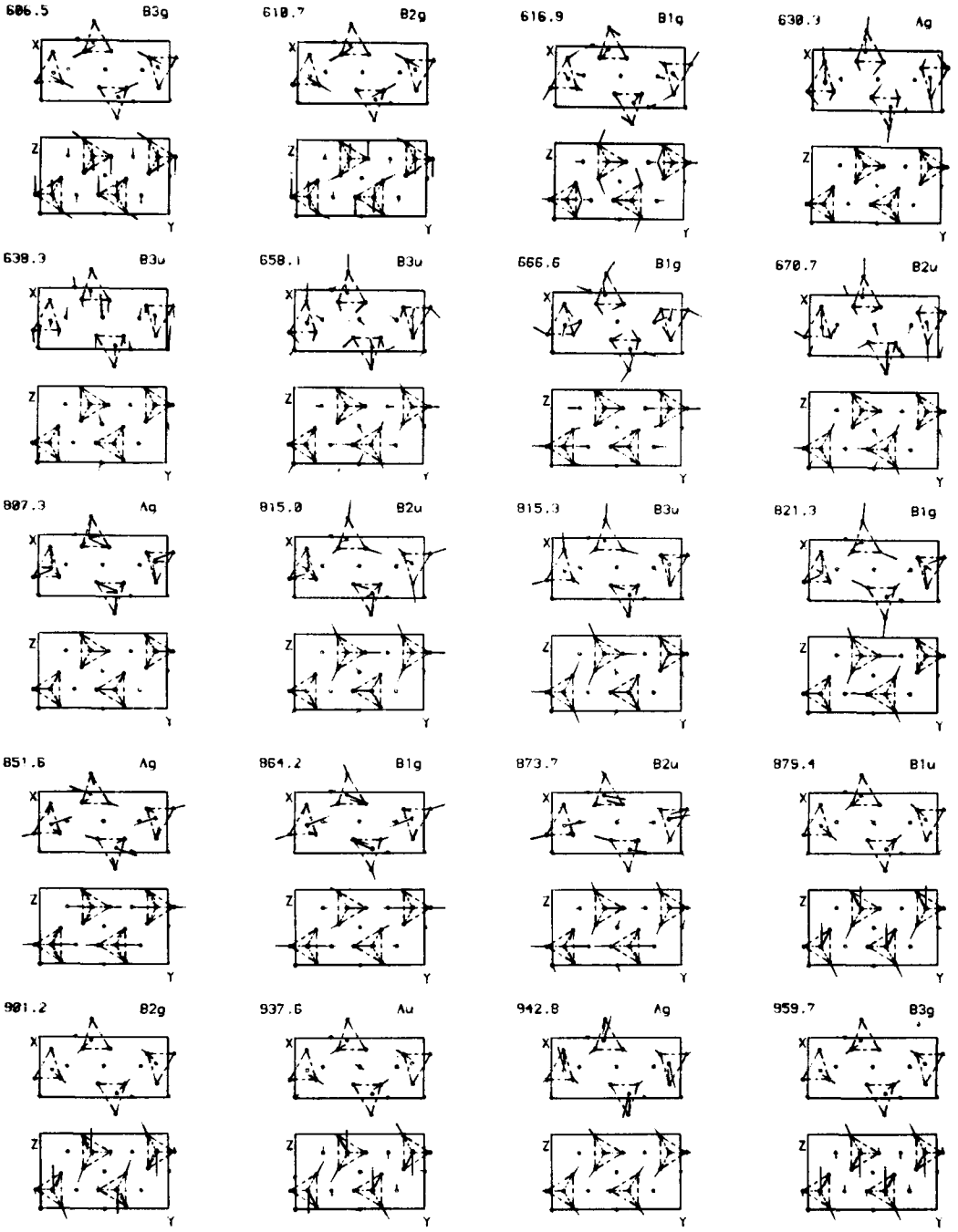
606.5 B3g
618.7 B2g
616.9 B1g
630.3 Ag
638.3 B3u
658.1 B3u
666.6 B1g
670.7 B2u
807.3 Ag
815.0 B2u
815.3 B3u
821.3 B1g
851.6 Ag
864.2 B1g
873.7 B2u
879.4 B1u
901.2 B2g
937.6 Au
942.8 Ag
959.7 B3g

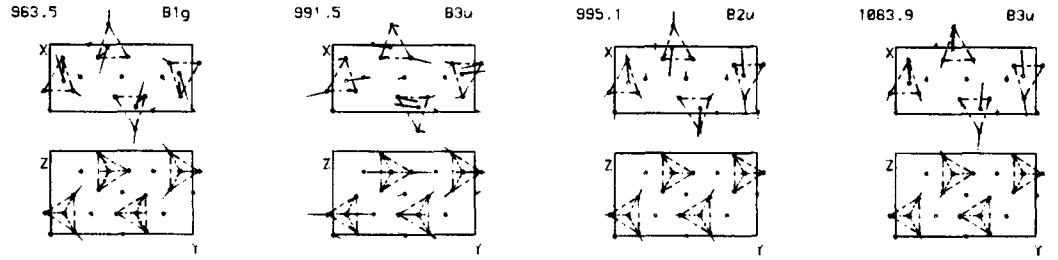

to another. We believe that the bond-bending or quasi-three-body terms in potential THB1 model the real effect of bond directionality in silicates, and that the inclusion of such terms in silicate potentials is both a major and vital development. The fact that the potential THB1 reproduces the known $\mathbf{q} = 0$ lattice dynamics of forsterite leads us to expect that it will also accurately predict the phonon dispersion, heat capacity, Gruneisen parameters, thermal expansion coefficients and the other bulk thermodynamic properties of forsterite, which are currently being investigated. We believe that our work has established the previously elusive quantitative link between the microscopic and macroscopic behaviour of the major Earth-forming mineral forsterite.

Acknowledgements

The authors would like to thank Prof. C. R. A. Catlow for his support and advice during the course of this and previous investigations. GDP gratefully acknowledges the receipt of a 1983 University Research Fellowship from the Royal Society.

References

Born, M., and Huang, K. (1954) *Dynamical theory of crystal lattices.* Clarendon Press, Oxford.

Burnham, C. W. (1985) In *Microscopic to Macroscopic.* Reviews in Mineralogy, **14** (Kieffer, S. W., and Navrotsky, A., eds.) Mineral Soc. Am. Washington.

Busing, W. R. (1981) *WMIN, a computer program to model molecules and crystals in terms of potential energy functions.* Oak Ridge National Laboratory, Oak Ridge.

Catlow, C. R. A. (1977) *Proc. R. Soc. London,* **A353,** 533–61.

——and Mackrodt, W. C. (1982) In *Computer simulations of solids.* Lecture notes in physics, 166 (Catlow, C. R. A., and Mackrodt, W. A., eds.) Springer-Verlag, Berlin.

——Doherty, M., Price, G. D., Sanders, M. J., and Parker, S. C. (1986) *Mater. Sci. Forum,* **7,** 163–76.

Cochran, W. (1973) *The dynamics of atoms in crystals.* Edward Arnold, London.

Devarajan, V., and Funck, E. (1974) *J. Chem. Phys.* **62,** 3406–11.

Iishi, K. (1978) *Am. Mineral.* **63,** 1198–208.

Kieffer, S. W. (1979*a*) *Rev. Geophys. Space Phys.* **17,** 1–19.

——(1979*b*) Ibid. **17,** 20–34.

——(1979*c*) Ibid. **17,** 35–58.

——(1985) In *Microscopic to Macroscopic.* Reviews in Mineralogy, **14** (Kieffer, S. W., and Navrotsky, A., eds.) Mineral. Soc. Am. Washington.

——and Navrotsky, A. (1985) *Microscopic to Macroscopic.* Reviews in Mineralogy, **14.** Mineralogical Soc. America, Washington.

Lazarev, A. N. (1974) In *The infrared spectra of Minerals* (Farmer, V. C., ed.) Mineralogical Society, London.

Lewis, G. V. (1985) *Physica,* **B131,** 114–18.

Matsui, M., and Busing, W. R. (1984) *Am. Mineral.* **69,** 1090–5.

——and Matsumoto, T. (1985) *Acta Crystallogr.* **B41,** 377–82.

McMillan, P. (1985) In *Microscopic to Macroscopic.* Reviews in Mineralogy, **14** (Kieffer, S. W., and Navrotsky, A., eds.) Mineral. Soc. Am. Washington.

Paques-Ledent, M. T., and Tarte, P. (1973) *Spectrochim. Acta,* **A29,** 1007–16.

Piriou, B., and McMillan, P. (1983) *Am. Mineral.* **68,** 426–43.

Price, G. D., and Parker, S. C. (1984) *Phys. Chem. Minerals,* **10,** 209–16.

————and Yeomans, J. (1985) *Acta Crystallogr.* **B41,** 231–9.

Sanders, M. J., Leslie, M., and Catlow, C. R. A. (1984) *J. Chem. Soc., Chem. Comm.* 1271–3.

Servoin, J. L., and Piriou, B. (1973) *Phys. Status Solidi,* (b)**55,** 677–86.

Ziman, J. M. (1964) *Principles of the theory of solids.* C.U.P., Cambridge.

[*Manuscript received 26 March; revised 28 May 1986*]